Influence of Preparation Method on the Metal Cluster Size of Pt/ZSM-5 Catalysts As Studied with Extended X-ray Absorption Fine Structure Spectroscopy

F. W. H. Kampers,[†] C. W. R. Engelen,[‡] J. H. C. van Hooff, and D. C. Koningsberger*

Laboratory for Inorganic Chemistry and Catalysis, Eindhoven University of Technology, P.O. Box 513, 5600 MB Eindhoven, The Netherlands *(Received: April 27, 1989; In Final Form: May 16, 1990)*

The size of Pt particles introduced into the channels of ZSM-5 zeolite by two different preparation methods has been studied with EXAFS. ZSM-5 was loaded with 2 wt % Pt by ion exchange and by impregnation. By careful calcination of the catalysts the dispersion was maintained. The EXAFS measurements were performed on the reduced system. Analysis of the data showed that in the impregnated sample the platinum was present in particles which on average were smaller than the platinum particles in the ion-exchanged sample. These results corroborate earlier high-resolution electron microscopy measurements performed ex situ on the calcined catalysts. Moreover, the average particle size found from EXAFS analysis agrees well with the HREM results, indicating that dispersion is maintained during reduction. Both techniques indicate particles that exceed the dimensions of a zeolite cage at the intersection of the channels. The fact that the impregnated system has smaller platinum particles than the ion-exchanged catalyst can be explained by the presence of additional potassium species in the pores of the impregnated zeolite. These species inevitably will hinder the migration of platinum to form larger particles.

Introduction

Zeolites consist of an aluminosilicate framework with a pore structure of intersecting channels. The pore structure of zeolites limits the size of the molecules entering and exiting the internal zeolite structure. In that way the product distribution of reactions taking place inside the pores of the zeolite is strongly dependent upon the size of the pores (ranging from 2.6 to 7.4 Å) (shape selectivity). Furthermore, the formation of large organic molecules which reduce the activity of catalytic systems with time (coking) is inhibited,[1,2] resulting in extended lifetimes of the catalysts.

The porous structure of zeolites with large intracrystalline volumes and high surface areas per unit weight can be used to support catalytic active material. In this way a bifunctional catalyst can be obtained which combines the catalytic properties of the zeolite, including the sieve function, with the properties of the introduced catalytic material. The preparation of a ZSM-5 zeolite with platinum particles introduced in the pore system has been reported by Dessau.[3] The cations neutralizing the negative charge of the aluminum sites were exchanged with $[Pt(NH_3)_4]^{2+}$, which was subsequently thermally decomposed. Competitive hydrogenation of linear and branched olefins was used to test the shape selectivity of the catalyst and thereby determine whether the platinum particles were intra- or extrazeolitic. Only slowly heating in oxygen to 350 °C prior to reduction resulted in well-dispersed platinum-on-zeolite catalysts with shape-selective properties.

A second method to introduce platinum in the pores is to impregnate the zeolite with a solution of $Pt(NH_3)_4(OH)_2$.[4] However, since only one platinum tetraammine complex can be associated with an aluminum site, atomic dispersion of the complexes inside the pores is expected with ion exchange, whereas the impregnation complexes will randomly be deposited in the zeolite pores. Furthermore, the platinum tetraammine complexes deposited by impregnation are neutral and therefore more mobile than the Coulomb bound $[Pt(NH_3)_4OH]^+$ species in ion-exchanged catalysts. For these reasons it was expected that ion exchange would produce more dispersed platinum and consequently smaller particles in ZSM-5 than impregnation.

Platinum on zeolite catalysts prepared by ion exchange and impregnation were characterized by Engelen[4,5] using thermogravimetric analysis, temperature-programmed decomposition, measurement of the propane conversion activity, and high-resolution electron microscopy. These experiments indicated that decomposition of the platinum tetraammine complex in the presence of oxygen produced small platinum oxide particles which were mainly located inside the pores of the zeolite. For the impregnated sample, indications of larger particles on the outside of the zeolite crystallites were also found. Surprisingly, HREM measurements on the calcined systems showed smaller internal particles for the impregnated sample than for the ion-exchanged sample.

To verify these remarkable conclusions, to research the possibility of the existence of a bimodal Pt particle size distribution, and to investigate the structure of the catalysts after reduction, in situ EXAFS measurements under hydrogen were carried out on 2 wt % platinum on ZSM-5 catalysts, prepared by ion exchange and by impregnation. The results of the analysis of these EXAFS measurements will be presented here. They corroborate the HREM conclusions that in the impregnated system the platinum particles are smaller than in the ion-exchanged catalyst.

Experimental Section

The synthesis of the ZSM-5 zeolite has been reported by Engelen.[5] Both samples were prepared from the potassium-ZSM-5 zeolite with a Si/Al ratio of 75 which was dried in air at 300 °C before use. The impregnated sample was prepared by the incipient wetness method. A small amount (0.33 g) of a $Pt(NH_3)_4(OH)_2$ solution containing 6 wt % Pt was added to 1 g of zeolite and left to dry in air. In the case of the ion-exchanged sample 1 g of zeolite was added to 0.33 g of the platinum tetraammine solution which was diluted with 10 g of doubly distilled water. The ion exchange took place overnight in the stirred solution. It was verified that afterwards no platinum was left behind in the solution. The solution was then filtered, rinsed with a small amount of water, and left to dry in air. Both catalysts were loaded with 2 wt % Pt. Small amounts of the samples (0.15 g) were cautiously calcined in a He/O_2 (4:1) flow of 150 mL/min with a heating rate of 1 °C/min from room temperature upto 300 °C. To quickly remove H_2O and NH_3 formed in the calcination process, a vertical reactor of 10 mm inner diameter was used in which the catalysts were packed in a very thin bed (1-2 mm).

For the EXAFS measurements the samples were pressed in a sample holder forming a self-supporting wafer with an absorbance

* To whom correspondence should be addressed.
[†] DLO/TFDL Technical and Physical Engineering Science for Agricultural Research, P.O. Box 356, 6700 AJ Wageningen, The Netherlands.
[‡] EXXON Chemicals Holland B.V., P.O. Box 7335, 3000 HH Rotterdam, The Netherlands.

(1) Post, J. G. "The Characterization of ZSM-5". Thesis, Eindhoven University of Technology, 1984.
(2) Biddy, D. M.; Milestone, N. B.; Patterson, J. E.; Aldridge, L. P. *J. Catal.* **1986**, *97*, 493.
(3) Dessau, R. M. *J. Catal.* **1984**, *89*, 520.
(4) Engelen, C. W. R.; Wolthuizen, J. P.; van Hooff, J. H. C.; Zandbergen, H. W. *Proc. 7th Int. Zeolite Conf.* **1986**, 709.
(5) Engelen, C. W. R. "Acid and Metal Catalysis with Zeolite ZSM-5". Thesis, Eindhoven University of Technology, 1986.

0022-3654/90/2094-8574$02.50/0

of about 2.5 at the Pt L_{III} edge and mounted in an in situ transmission cell.[6] The samples were dried at a temperature of 100 °C under a He flow of 100 mL/min before reduction at 350 °C in a flow of 100 mL/min H_2 (heating rates 5 °C/min).

The Pt L_{III} EXAFS measurements on the samples were performed on station 8.1 of SRS (Daresbury, UK) at liquid nitrogen temperatures in a hydrogen atmosphere. The ring was operated at an energy of 2 GeV with the current typically in the 100–200-mA range. A bent Si(220) double crystal monochromator was used and the second crystal was detuned to 50% of the maximum intensity for higher harmonic rejection. Ionization chamber detectors stationary filled with a mixture of argon and helium were employed to monitor the incoming and transmitted flux. The Ar/He gas mixture was chosen to give 20% absorption in the I_i chamber and 80% in the I_t chamber.

Experimental phase and backscattering amplitude functions were derived from platinum foil data (thickness 4 μm) measured at SRS (Daresbury, UK), station 9.2 (beam conditions: 2 GeV, 130–90 mA and the wiggler at 5 T). A flat double crystal Si(220) monochromator was used with 50% harmonic rejection. The gas fillings of the I_i and I_t ionization chambers were equivalent to those of the measurements on the zeolite samples. The foil was kept at liquid nitrogen temperature during the measurement. The transferability of the data from station 9.2 to 8.1 was verified by analyzing Pt foil data measured at room temperature on 8.1 with phase and backscattering amplitude functions extracted from 9.2 foil data also measured at room temperature.

Data Analysis and EXAFS Results

Standard data reduction procedures[7] have been employed to isolate the EXAFS oscillations from the raw EXAFS spectra. In Figure 1 the χ's of the foil (a) and of the ion-exchanged (c) and impregnated (e) samples are shown together with the k^3 Fourier transforms (b, d, and f, respectively).

From the crystallographic data[8] of bulk fcc platinum, coordination numbers and coordination distances of near-neighbor shells can be derived. Phase and backscattering amplitude functions of the Pt–Pt absorber–backscattering pair may be derived from the back transformation of the first shell. The atoms in the fourth shell are shadowed by the atoms in the first shell, resulting in multiple scattering effects. Consequently the EXAFS of this shell is amplified and an additional phase factor is introduced. This shell will therefore have phase and amplitude functions which differ from the ones of a normal Pt–Pt absorber–backscatterer pair.[9-11]

In order to check the presence of a bimodal size distribution of the platinum particles—which involves the estimation of three parameters (average size of both types of particles and the amount of platinum in the particles of one of the types relative to the other)—the coordination numbers of at least three shells must be determined accurately.[12] A complicating factor in the data analysis is the relatively small coordination number of the second shell combined with the fact that this shell in a Fourier transform overlaps with the side lobes of the peak of the first shell.

The conventional method of analysis involves a back transformation of the first shell of the Pt foil data to extract the phase and amplitude functions of the Pt–Pt absorber–scatterer pair. Ideally a reference compound should have only one coordination shell, which can than be backtransformed over a large R space window. In practice this is never the case and a limited window is used to separate the absorber–scatterer pair shell from other

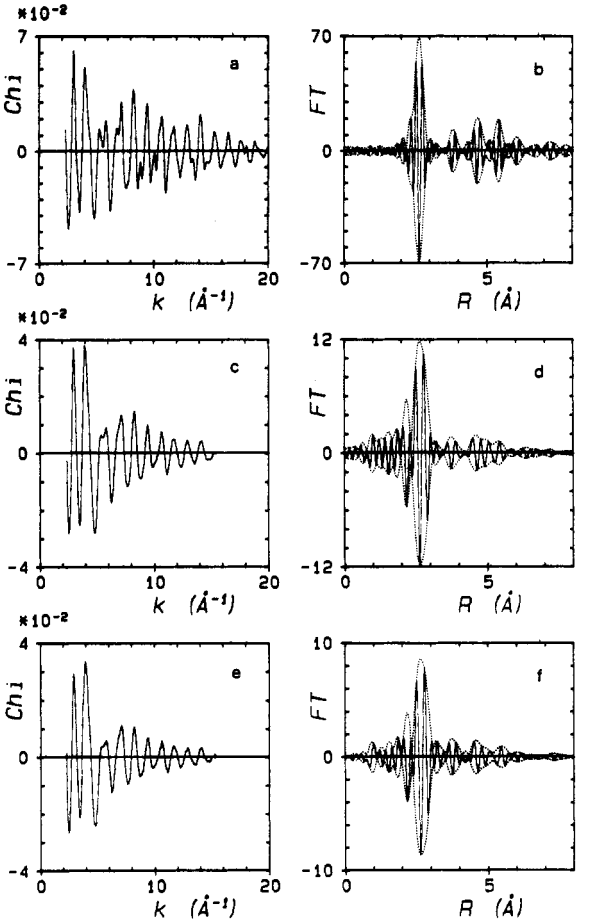

Figure 1. EXAFS functions and k^3 Fourier transforms of the Pt foil (a and b) (FT range 2.30–19.87 Å^{-1}), of the 2 wt % Pt/ZSM-5 sample prepared with ion exchange (c and d) (FT range 2.72–15.19 Å^{-1}) and of the 2 wt % Pt/ZSM-5 impregnated sample (e and f) (FT range 2.20–14.95 Å^{-1}).

shells. The back transformation window, however, has a large influence on the size and shape of the side lobes of the Fourier transform of a calculated shell. In this case it makes a reliable determination of the coordination parameters of the second shell impossible, unless a method can be found to extract the phase and backscattering amplitude functions more accurately from the Pt foil data. We devised a two-stage method which involves elimination of neighboring shells by estimating them with preliminary phase and backscattering amplitude functions and subtracting them from the reference compound data. The result is an EXAFS spectrum of an almost ideal reference compound. The errors introduced by the use of preliminary phase and backscattering amplitude functions are of second order since the neighboring shells in the Pt foil data are an order of magnitude smaller than the main peak used to extract the phase and amplitude functions. (Iteratively improving the quality of the phase and backscattering amplitude functions should be disadvised since the method decreases the k range of the reference spectrum.)

The phase and amplitude functions for both the Pt–Pt pair and the Pt–(Pt)–Pt combination of the fourth shell were thus extracted from the foil data in two stages. First, preliminary phase and backscattering amplitude functions were calculated from the inverse Fourier transforms of the first (R range 1.72–3.40 Å) and fourth shell (R range 5.18–5.64 Å) in the k^3 Fourier transform of the Pt foil EXAFS (k range 2.30–19.87 Å^{-1}). These functions were than used to model the first five coordination shells in the Pt foil data in R space. Unfortunately, because the coordination number N and the Debye–Waller factor $\Delta\sigma^2$ and the coordination distance R and the relative inner potential correction ΔE_0 of one shell are correlated, different combinations of N and $\Delta\sigma^2$ and R and ΔE_0 give equally good matches in R space. To decouple the parameters, use must be made of the fact that the influence of

(6) Kampers, F. W. H.; Maas, T. M. J.; van Grondelle, J.; Brinkgreve, P.; Koningsberger, D. C. *Rev. Sci. Instrum.* **1989**, *60*, 2635.
(7) van Zon, J. B. A. D.; Koningsberger, D. C.; van't Blik, H. F. J.; Sayers, D. E. *J. Chem. Phys.* **1985**, *82*, 5742.
(8) Wyckoff, R. W. G. *Crystal Structures*, 2nd ed.; Wiley: New York, 1963.
(9) Stern, E. A. In *X-ray Absorption*; Koningsberger, D. C., Prins, R., Eds.; Wiley: New York, 1988; p 45.
(10) Teo, B. K. *J. Am. Chem. Soc.* **1981**, *103*, 3990.
(11) Stern, E. A.; Bunker, B. A.; Heald, S. M. *Phys. Rev. B* **1980**, *21*, 5521.
(12) Greegor, R. B.; Lytle, F. W. *J. Catal.* **1980**, *63*, 476.

TABLE I: Results of the Modeling of the First Four Shells of Pt Foil Data and Comparison with the Coordination Parameters of Bulk fcc Platinum Derived from Ref 8

shell	N'	N_{ref}	R, Å	R_{ref}, Å	$\Delta\sigma^2$, Å^2	ΔE_0, eV	reference
1	11.9	12	2.77	2.77	0	0	Pt–Pt
2	4.8	6	3.92	3.92	0.00015	−6.5	Pt–Pt
3	14.3	24	4.78	4.80	0.0009	0.5	Pt–Pt
4	10.4	12	5.55	5.54	−0.0005	0	Pt–(Pt)–Pt

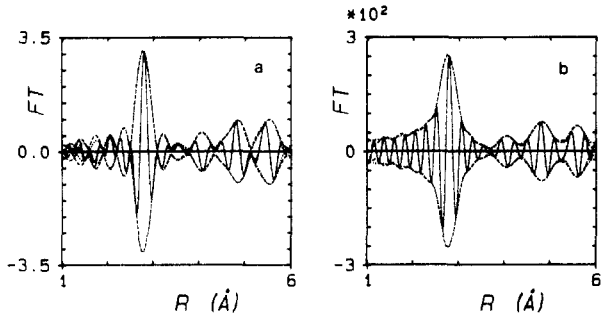

Figure 2. Phase and backscattering amplitude corrected k^1 (a) and k^3 (b) Fourier transforms of the original Pt foil data (---, absolute part; —, imaginary part) and of the model EXAFS data calculated by using the coordination parameters of Table II (···, absolute part; – –, imaginary part). Range in k space: 3.19–13.85 Å^{-1}.

$\Delta\sigma^2$ and ΔE_0 is not the same for different k regions whereas N and R act similarly on the whole k range. By comparing both the k^1 and k^3 weighted Fourier transforms of the calculated data with the similarly Fourier transformed measured data (using the same k interval) and optimizing the coordination parameters used in the calculation to yield a good fit in both k^1 and k^3 transforms, we can find unique values for the parameter pairs N and $\Delta\sigma^2$ and R and ΔE_0.[13] Since the parameters are now decoupled, a good fit in both k^1 and k^3 also means that the calculated spectrum will fit the measured spectrum in k space. The advantage of this method is that the fit of individual shells can be judged while simultaneously the influence of a change in the coordination parameters of one shell on the fit of neighboring shells can be monitored.

The parameters found from analysis of the first five shells of the Pt foil data were used to calculate the EXAFS functions of the second, third, and fifth shells. These EXAFS functions were then subtracted from the original EXAFS, resulting in the EXAFS function of only the first and fourth cells. From the Fourier transform of this data (k range 2.73–19.26 Å^{-1}) the shells could be backtransformed over a wider range. The absence of overlap between neighboring shells results in better phase and backscattering amplitude functions. For the first shell back transformation was done from 1.32 to 3.72 Å while for the fourth shell the R range was 4.90–5.98 Å.

Unfortunately the spectra of the samples were not measured over the same energy range as for Pt foil. Therefore, the usable data range of the Pt/ZSM-5 samples in k space is shorter than the data range of the foil. This will drastically affect the Fourier transforms. Furthermore, from the EXAFS formula[14] it is obvious that the amplitude of the EXAFS of a particular shell, via the mean-free-path term, is a function of R. Modeling coordination shells at R values which differ from the radius of the coordination shell from which the phase and amplitude functions were calculated results in erroneous coordination numbers. The coordination numbers found from analysis haveto be corrected by using $N_j = N'_j \exp(2(R_j - R_{ref})/\lambda)$ in which N'_j is the coordination number of the jth shell found from analysis, N_j is the corrected coordination number, R_j is the radius of the jth coordination shell, R_{ref} is the radius of the shell used for the extraction of the phase and backscattering amplitude functions, and λ is the mean free path.

(13) Kampers, F. W. H. "EXAFS in Catalysis, Instrumentation and Applications". Thesis, Eindhoven University of Technology, 1988.
(14) Boland, J. J.; Crane, S. E.; Baldeschwieler, J. D. *J. Chem. Phys.* **1982**, *77*, 142.

TABLE II: Results of the Modeling of the First Four Shells of the Data of the 2 wt % Pt/ZSM-5 Sample Prepared with Ion Exchange

shell	N'	N	R,[a] Å	$\Delta\sigma^2$,[b] Å^2	ΔE_0,[b] eV	reference
1	8.8[b]	8.8[b]	2.77	0.0030	1.6	Pt–Pt
2	3.1[c]	3.9[c]	3.93	0.0051	−6.9	Pt–Pt
3	7.1[b]	12[b]	4.76	0.0055	2.6	Pt–Pt
4	3.7[c]	3.7[c]	5.51	−0.0020	3.0	Pt–(Pt)–Pt

[a] Accuracy ±1%. [b] Accuracy ±20%. [c] Accuracy ±30%.

TABLE III: Results of the Modeling of the First Three Shells of the Data of the Impregnated 2 wt % Pt/ZSM-5 Sample

shell	N'	N	R,[a] Å	$\Delta\sigma^2$, Å^2	ΔE_0, eV	reference
1	7.2[b]	7.2[b]	2.77	0.0034	1.4	Pt–Pt
2	2.8[c]	3.5[c]	3.91	0.0072	−4.5	Pt–Pt
3	3.8[b]	6.4[b]	4.79	0.0043	−0.3	Pt–Pt

[a] Accuracy ±1%. [b] Accuracy ±20%. [c] Accuracy ±30%.

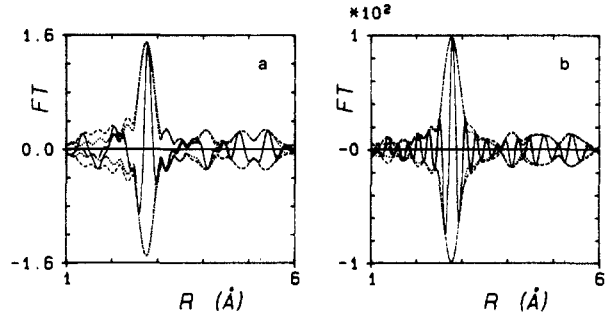

Figure 3. Phase and backscattering amplitude corrected k^1 (a) and k^3 (b) Fourier transforms of the data of the 2 wt % ion-exchanged Pt on ZSM-5 sample (---, absolute part and —, imaginary part) and of the model calculated from the coordination parameters of Table III (···, absolute part; – –, imaginary part). Range in k space: 3.14–13.76 Å^{-1}.

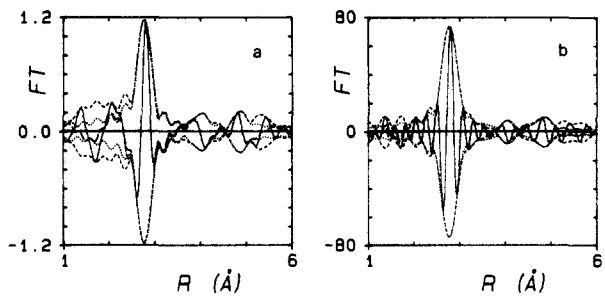

Figure 4. Phase and backscattering amplitude corrected k^1 (a) and k^3 (b) Fourier transforms of the data of the 2 wt % impregnated Pt on ZSM-5 sample (---, absolute part; —, imaginary part) and of the model calculated from the coordination parameters of Table IV (···, absolute part and – –, imaginary part). Range in k space: 3.13–13.79 Å^{-1}.

In order to compensate for these effects, the first four coordination shells of Pt in the foil data once again were modeled in R space, employing the method described above. The Fourier transform range in k space now used was comparable to the k range of the samples. The results are presented in Table I; Figure 2 compares the models in R space with the original data for both k^1 and k^3 Fourier transforms. The accuracy with which these parameters have been determined is higher than the normal EXAFS accuracies because many of the errors introduced in standard analysis, e.g., deviations in normalization, differences in background subtraction or inaccuracies in edge position determination, are compensated by the fact that phase and amplitude functions were derived from and applied to the same data file. The results given in Table I indicate that the mean free path λ is 10 Å for the second shell and 8 Å for the third shell. These values are well within the range of mean-free-path values given by Lindau and Spicer.[15]

(15) Lindau, I.; Spicer, W. *J. Electron Spectrosc. Relat. Phenom.* **1974**, *3*, 409.

The EXAFS data of the Pt/ZSM-5 samples were also analyzed with the method described above. Model EXAFS functions were calculated from proposed coordination parameters of several shells by using the appropriate phase and backscattering amplitude functions. The individual EXAFS functions were added and the proposed coordination parameters optimized by comparing the k^1 and k^3 Fourier transforms of model and experimental data in R space. Tables II and III list the best fit coordination parameters obtained in this way for the data of the ion-exchanged sample and the impregnated sample, respectively. The quality of the coordination parameters can be judged from the Figures 3 and 4, respectively. The fourth shell of the EXAFS data of the impregnated sample could not be modeled to yield acceptable coordination parameters. For that reason the fourth shell was not considered in quantitative comparisons between both samples.

As was pointed out above, the coordination numbers found from analysis still have to be corrected for the R dependence of the EXAFS amplitude with the results of the analysis for the Pt foil data. For the second and third shell, the correction is expressed by

$$N_j = N'_j\left(\frac{N_{j,\mathrm{ref}}}{N'_{j,\mathrm{ref}}}\right)^{(R_j-R_{\mathrm{ref}})/(R_{j,\mathrm{ref}}-R_{\mathrm{ref}})} \quad (1)$$

in which N_j is the corrected coordination number of the jth shell, N'_j is the coordination number found from analysis (Tables II and III), $N'_{j,\mathrm{ref}}$ the coordination number found from the analysis of the data of the Pt foil (Table I), and $N_{j,\mathrm{ref}}$ the coordination number is the bulk, known from crystallographic sources. Similarly, R_j is the coordination distance found from analysis of the sample, $R_{j,\mathrm{ref}}$ the distance found from the analysis of the foil data, and R_{ref} the crystallographic distance used to obtain the phase and backscattering amplitude functions. Tables II and III also list the corrected coordination numbers of the first three shells of the samples.

The accuracy of the coordination number of the second shell is less than the accuracy with which the coordination numbers of the first and third shells have been determined because the intensity of the second shell is considerably smaller than that of the other two. Furthermore, the position of the shell in R space coincides with the position of the first side lobe of the large first-shell peak. Within the accuracy of EXAFS no indication of Pt–O absorber–backscatterer pairs was found in the spectra of either of the samples.

Discussion

The coordination distances found above and the electron microscopy investigations reported by Kleine et al.[16] suggest that the platinum in ZSM-5 is present in particles having fcc structure. The HREM investigations of these catalysts reported by Engelen[5] and by Zandbergen et al.[17] indicate that the particles are spherical.

Coordination parameters found from EXAFS analysis are averages of the coordination parameters of all individual platinum atoms in the irradiated volume of the sample. If the platinum atoms are present in particles, the average coordination number is a function of particle size. From model calculations in which consecutive atoms were placed in those vacant fcc lattice positions that were closest to the center of mass of the particle, the behavior of the average coordination number as a function of the number of atoms in the particle for the first three shells in a spherical fcc particle has been derived (Figure 5). Figure 5 can be used to estimate the number of atoms in the particle from the coordination numbers of Tables II and III.

As has already been mentioned, investigation of a bimodal particle-size distribution involves the calculation of three unknown parameters: the average size of the small particles, the average size of the large particles, and the amount of platinum in the small

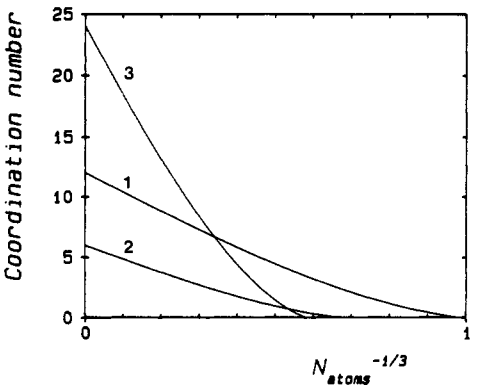

Figure 5. Average coordination number of the first three shells of atoms in spherical particles with an fcc structure, as a function of the number of atoms in the particle.

TABLE IV: Number of Atoms and Particle Diameters Derived from the Coordination Numbers of Tables II and III

	ion exchange		impregnation	
shell	n_{atoms}	D,[a] Å	n_{atoms}	D,[a] Å
1	130[b]	18	40[b]	13
2	160[c]	19	90[c]	16
3	90[b]	16	20[b]	11

[a] Accuracy 10%. [b] Accuracy 50%. [c] Accuracy 70%.

particles relative to the amount of platinum in the large particles. This can only be done if the coordination numbers of at least three shells can be determined accurately. The large inaccuracy in the estimates of Table IV, especially of the second shell, therefore does not allow conclusions about the size distribution of the particles as could recently be done by Bein et al. for Ni in Y zeolite.[18] However, since the estimates from the first and third shell, the shells that could be determined best, do not diverge much, it can be excluded that a significant fraction of platinum is present in (external) much larger particles as was proposed by Engelen.[5] In that case these two shells can be used to calculate average values for the number of atoms per particle: in the ion-exchanged system an average Pt atom resides in a particle containing 110 ± 50 atoms, whereas in the impregnated system it resides in particle of 30 ± 10 Pt atoms. From the model calculations, the diameter of these particles, approximated by 2 times the distance from the last added atom to the center of mass plus the atomic diameter, could be estimated to be 17 ± 2 Å for the ion-exchanged samples and 12 ± 1 Å for the impregnated sample. Note that these values are derived from the EXAFS determined environment of the average Pt atom. In case of a broad distribution of particle sizes these values are biased toward larger particles containing greater numbers of atoms relative to direct determination of particle size (e.g., microscopy).

The decomposition of the platinum tetraammine complex was done in the presence of oxygen to immobilize the platinum in the polar PtO_2 phase, as was first proposed by Dalla Betta and Boudart[19] for Y zeolite and Dessau[3] for ZSM-5 and recently verified by Shoemaker and Apple for ruthenium in Y zeolite.[20] The HREM investigations performed on the calcined samples after decomposition of the $[Pt(NH_3)_4]^{2+}$ complex indicate a PtO_2 particle size range of 8–25 Å for the ion-exchanged sample while for the impregnated sample particles of about 10 Å were observed.[5] Comparison of the HREM results on the calcined catalysts with the in situ EXAFS results of the reduced systems shows that the dispersion of the platinum particles is maintained during reduction at 350 °C. In light of the inherent difference in the average

(16) Kleine, A.; Ryder, P. L.; Jaeger, N.; Schulz-Ekloff, G. *J. Chem. Soc., Faraday Trans. 1* **1986**, *82*, 205.
(17) Zandbergen, H. W.; Engelen, C. W. R.; van Hooff, J. H. C. *Appl. Catal.* **1986**, *25*, 231.
(18) Bein, T.; McLain, S. J.; Corbin, D. R.; Farlee, R. D.; Möller, K.; Stucky, G. D.; Woolery, G.; Sayers, D. E. *J. Am. Chem. Soc.* **1988**, *110*, 1801.
(19) Dalla Betta, R. A.; Boudart, M. In *Proceedings of the 5th International Congress on Catalysis, Palm Beach, 1972*; North Holland: Amsterdam, 1973; Vol. 2, p 1329.
(20) Shoemaker, R.; Apple, T. *J. Phys. Chem.* **1987**, *91*, 4024.

particle size as determined by these methods as described above, this close agreement suggests a narrow distribution of particle sizes, diminishing the relative biases in the values derived from the environment of the average Pt atom.

The cages at the intersections of channels in ZSM-5 zeolite have a diameter of about 7 Å[21] and can accommodate particles containing upto about 20 atoms.[5] As both HREM and EXAFS indicate that the particles contain appreciably more atoms, it must therefore be concluded that the zeolite lattice is locally damaged by the particles. This has previously been reported for Y zeolites[22-24] and also for ZSM-5.[24] From the fact that the overall zeolite structure as observed in HREM is not damaged, it is commonly agreed that the damage is restricted to the immediate vicinity of the metal particle and that the structure of the zeolite crystallite—and thereby the shape selectivity—remains intact.

The fact that no Pt–O bonds are observed can be explained by the small number of such bonds per platinum atom in N particles of these sizes. Furthermore, it is likely that the platinum atoms constituting the particles are randomly distributed with respect to the zeolite lattice. Finally, in a locally disrupted zeolite lattice ordered Pt–O bonds will not be present anymore.

A possible explanation for the paradoxical result that impregnation yields smaller particles that ion exchange might be found in the presence of potassium. The Si/Al ratio of 75 used here corresponds to 1.3 negative sites per unit cell. Charge neutrality requires an equal amount of potassium cations. A loading of 2 wt % Pt corresponds to 0.6 Pt atoms per unit cell. At the end of the ion-exchange procedure, the concentration of platinum complexes in solution is zero. This indicates that the exchange reaction of K^+ for $[Pt(NH_3)_4OH]^+$ is favored over the reaction in the other direction. Naturally this will also be true if the solution is impregnated in the pores. Consequently, regarding the platinum complexes both techniques are equivalent and will result in catalytic systems in which about 50% of the potassium cations are exchanged for $[Pt(NH_3)_4OH]^+$ ions. However, in the ion-exchanged system the liberated potassium ions will diffuse out of the zeolite because of a concentration gradient whereas with impregnation these ions will randomly be deposited in the pores of the zeolite structure in the drying process. Therefore, apart from the formation of potassium cations and platinum tetraammine complexes, bound by a Coulomb interaction to the aluminum sites, impregnation will result in the random deposition of neutral potassium hydroxide groups in the pores.

During calcination the platinum tetraammine complexes are decomposed and platinum oxide is formed in combination with protons or ammonium ions which neutralize the negative charge of the aluminum sites. The polar platinum oxide molecules have limited mobility because they have dipole–dipole interactions with the zeolite lattice. In the impregnated system additional potassium species will be present which, because of their polarity, also have reduced mobility. Results of Tzou et al.[25,26] and Jiang et al.[27] indicate that irreducible species—in their case Fe^{2+}—can reduce sintering of platinum particles in Y zeolite. In both samples discussed here, irreducible cationic species are present in the form of K^+ ions electrostatically bonded to the aluminum sites which possibly can act as chemical anchors for platinum metal particles. The impregnated sample, however, has additional potassium hydroxide molecules which partially block the pores of the zeolite and thus reduce the ability of the platinum to migrate.

The fact that the pores of the zeolite are partially blocked will also affect the catalytic behavior of the systems. This has been observed by Engelen et al.[4] in the propane conversion as a function of time. The impregnated system shows a behavior which resembles a Pt/Al_2O_3 catalyst. This is consistent with the fact that due to the blocking of the pores by K_2O only the exterior Pt particles are accessible for reactants and/or that reaction products formed in the interior of a zeolite particle are hindered in their way out.

Conclusions

In situ EXAFS has been used to determine the average size of platinum crystallites in ZSM-5 zeolite prepared by ion exchange and impregnation. The experiments were performed in a hydrogen atmosphere after thermal decomposition of the platinum tetraammine complex in the presence of oxygen and subsequent reduction at 350 °C. Although the quality of the EXAFS data was insufficient to derive a size distribution for the crystallites from the coordination numbers of three nearest neighbor shells, it could be excluded that a significant fraction of platinum is present in large (external) particles and average particle sizes for both samples could reliably be established. It was found that the size of the particles in the impregnated sample was smaller than those in the sample prepared by ion exchange. This result, which corroborates previous HREM investigations on the same samples after the decomposition step, is explained by the presence of additional potassium hydroxide molecules in the impregnated sample blocking the pores of the zeolite.

The fact that the average particle sizes in the reduced Pt/ZSM-5 systems as determined with EXAFS agree with those of the unreduced catalysts as determined with HREM indicates that the dispersion is maintained during reduction.

Because the metal particles have average diameters which are 1.5–2 times larger than can be accommodated by a channel intersection cage of ZSM-5 it is concluded that the zeolite lattice is locally disrupted in the vicinity of the particles.

Registry No. Pt, 7440-06-4.

(21) Olson, D. H.; Kokotailo, G. T.; Lawton, S. L.; Meier, W. M. *J. Phys. Chem.* **1981**, *85*, 2238.
(22) Moraweck, B.; Renouprez, A. J. *Surf. Sci.* **1981**, *106*, 35.
(23) Gallezot, P.; Datka, J.; Massardier, J.; Primet, M.; Imelik, B. *Proceedings of the 6th International Congress on Catalysis, London*; Chemical Society: London, 1976; Vol. 2, p 696.
(24) Jaeger, N. I.; Schulz-Ekloff, G.; Svensson, A. In *New Developments in Zeolite Science and Technology*; Murakami, Y., Iijima, A., Ward, J. W., Eds.; Elsevier: Amsterdam, 1986; p 923.
(25) Tzou, M. S.; Jiang, H. J.; Sachtler, W. M. H. *Appl. Catal.* **1986**, *20*, 231.
(26) Tzou, M. S.; Jiang, H. J.; Sachtler, W. M. H. *React. Kinet. Catal. Lett.* **1987**, *35*, 207.
(27) Jiang, H. J.; Tzou, M. S.; Sachtler, W. M. H. *Appl. Catal.* **1988**, *39*, 255.